

## SPECTRAL ALBEDOS OF AN ALPINE SNOWPACK

Thomas C. Grenfell and Donald K. Perovich

*Department of Atmospheric Sciences, University of Washington, Seattle 98195 (U.S.A.)*

and John A. Ogren

*Department of Civil Engineering, University of Washington, Seattle 98195 (U.S.A.)*

(Received July 15, 1980; accepted in revised form September 22, 1980)

### ABSTRACT

*Spectral albedos ( $\alpha_\lambda$ ) from 380 to 2500 nm are reported for a snowpack in the Cascade Mountains of Washington. Data were obtained from just after an 0.4 m snowfall on 13 March 1980 until the pack had metamorphosed to melting coarse grains about 1 mm in diameter mixed with dust. Measurements were made under cloudy conditions to obtain a diffuse incident radiation field. Structural parameters of the snow were measured concurrently for all cases, and on three occasions, estimates of absorbing impurity content were obtained. The dependence of the spectral albedos of the snowpack on grain size and impurity content is illustrated. Comparison of wavelength-integrated albedos ( $\alpha_{obs}$ ) obtained using Kipp and Zonen radiometers with corresponding albedos derived from  $\alpha_\lambda$  data show good agreement, and suggests a correlation between  $\alpha_{obs}$  and the amount of incident radiation transmitted by the cloud layer. Comparison with theoretical models confirms that impurities in the snow depress  $\alpha_\lambda$  at visible wavelengths but have little effect beyond 900 nm in the infrared; however, quantitative agreement with theory is uncertain at present.*

### INTRODUCTION

Albedos of snow are important for determining the hydrological balance at mid to high latitudes and in mountainous regions, and for studying the

radiative energy balance of the Earth. Considerable variety exists in the literature regarding the albedos of snow surfaces. Reported values for wavelength-integrated albedos ( $\alpha$ ) range from approximately 0.93 for dry packed snow (Bryazgin and Koptev 1969) to about 0.63 for wet old snow (Grenfell and Maykut 1977). This variation is attributed to changes in a number of parameters, including the size and shape of the snow particles, the spectral and angular distribution of the incident radiation field, departures of the surface from a flat, optically thick, homogeneous layer, and impurities in the snow. Systematic differences may also arise from variations in the spectral or angular sensitivities of the detectors used. A comprehensive review of available albedo observations by Bohren and Barkstrom (1974) points out that while detailed measurements of the accompanying physical properties of the snow are necessary for interpreting these observations, such information is usually unavailable. Thus, the extent to which a particular set of data is influenced by the above-mentioned parameters is difficult to assess.

Recent work has been devoted to isolating the effects of these parameters on snow albedo. Grenfell and Maykut (1977) pointed out that to determine how  $\alpha$  is influenced by changes in the spectral distribution of the incident radiation, spectral albedos ( $\alpha_\lambda$ ) are needed. They calculate a decrease in  $\alpha$  for their melting old snow case from 0.77 under heavy overcast skies, to 0.63 for clear skies. Theoretical studies (Bohren and Barkstrom 1974, Choudhury 1979, Wiscombe and Warren 1980) suggest that for

pure snow the particle size is the controlling parameter and that the snow density is unimportant. Bohren and Beschta (1979) have confirmed that below  $0.5 \text{ g/cm}^3$ ,  $\alpha$  is nearly independent of density. The data of O'Brien and Munis (1975) indicate a strong dependence of spectral reflectance on snow ageing, grain texture, surface melting, and the angular distribution of the incident radiation field. Their results, however, give relative directional reflectances rather than albedos (defined here as upwelling irradiance at the surface divided by incident irradiance), and unfortunately, grain sizes for their samples are not given. Grenfell and Maykut (1977) and Kuhn and Siogas (1978) give spectral albedos of polar snow for a few sites, but they also do not quote grain sizes. A problem exists in the comparison between theoretical and observational results. Calculations of  $\alpha_\lambda$  give values at visible wavelengths, even for unrealistically large grain radii of 1 cm (Choudhury 1980), which are significantly larger than observations indicate (Grenfell and Maykut 1977, Kuhn and Siogas 1978, Mellor 1966), and although differences between theory and observation are fairly small, the albedos are so close to unity that even small differences represent large variations in the solar energy penetrating the snowpack at visible wavelengths. Only for measurements from remote areas where the snow is very clean (Liljequist 1956, Holmgren 1977) are observed values as large as predictions. For these reasons, Warren and Wiscombe (1980) suggest that in natural snow the concentration of impurities is usually high enough to give excess absorption which causes a measurable decrease in the albedo.

The object of the present experiment was (1) to obtain a set of observations to determine the evolution of the spectral albedo of a natural snowpack from initial snowfall until metamorphosis to granular melting snow, and (2) to measure the accompanying changes in the physical parameters specifying the state of the snow. Such results should allow a more accurate comparison between theory and observations for a variety of snow conditions, and should provide representative values for climatological studies.

## MEASUREMENTS

The observations were carried out in early spring 1980 at the 3000 foot level in the Cascade Mountains of Washington. Incident and reflected irradiances were obtained at 46 selected wavelengths between 400 and 2750 nm using a portable visible and infrared scanning photometer (Grenfell 1981). Data were taken only under fully overcast conditions to ensure a diffuse radiation field for all cases. To monitor changes in the radiation field due to fluctuations in the cloud cover, reference values of total incident solar irradiance were obtained using a Kipp and Zonen radiometer. Measurements of total upwelling irradiance were also made to provide integrated albedos for comparison with the spectral albedos. Concurrent observations of snow density were made with a Taylor-LaChapelle density kit, and grain sizes and geometry were observed using an American Optical 20 power eyepiece or a Wild microscope, depending on the required resolution. On three occasions, snow samples were obtained for later analysis of impurity content. The samples were taken from the top 100 mm of the snow to average over the layers to which the albedo is most sensitive. The optical observations were begun on 13 March after a new snowfall of 0.4 m thickness on the previous evening. Seven sets of data were taken over a period of 35 days as the snowpack evolved in response to the gradually increasing air temperature. Observations were discontinued when the snow particles had metamorphosed to granules 0.75 to 2 mm in diameter and the snow density had reached 0.5 to  $0.55 \text{ g/cm}^3$ , typical of melting spring snow.

The impurity content was determined in two stages. In the field, the snow was examined visually as described and, except on April 17, appeared to have no detectable concentration of particles greater than  $10 \mu\text{m}$  in size. For smaller particles the integrating plate method (Lin et al. 1973, Weiss et al. 1979, Sadler et al. 1981) was used to determine the particle absorption coefficient, from which the mass concentration of absorbing impurities was estimated. The melted snow samples were first passed through a  $5 \mu\text{m}$  nylon mesh to remove foreign contaminants (e.g., insects and pollen). The particulate matter was collected on a quartz fibre filter, and the particle absorption coefficient was deter-

mined by measuring the transmission of visible light (550 nm) through the filter before and after sampling. The absorption coefficient for urban aerosol is usually dominated by graphitic carbon (Rosen et al. 1979), although in some cases wind-blown mineral dust may be important. Because absorption by graphitic carbon is a weak function of wavelength in the visible whereas mineral dust shows a strong decrease with wavelength (Weiss et al. 1979), the wavelength dependence of absorption can be used to discriminate between the two cases. Spectral absorption tests on the samples obtained in this study showed a wavelength dependence close to  $\lambda^{-1}$ , indicating that mineral dust was not the dominant absorber. In order to allow comparison with the theoretical analysis of Warren and Wiscombe (1980), an assumed absorption efficiency of  $8 \text{ m}^2/\text{g}$  at 550 nm was used to infer the

mass concentration of impurities from measured absorption coefficients. This value is calculated for sub  $0.1 \mu\text{m}$  graphitic carbon particles by Bergstrom (1973), and is close to the results measured for acetylene smoke particles by Roessler and Faxvog (1980). The resulting impurity levels are given in Table 1. Although a detailed study of the overall accuracy of the present technique has not yet been performed, a preliminary evaluation of the uncertainties in the sample handling and analysis indicates an overall uncertainty in the absorption measurement of a factor of two to three. Useful results were obtained from the 18 March and 26 March experiments, indicating an increase in impurity content, although the difference between the two samples may not be significant.

The sample taken on 17 April was heavily loaded

TABLE 1

Physical data and integrated albedos for the snow

Case	Date	$T_{\text{air}}$	$z_{\text{snow}}$ (m)	Grain* radius (mm)	Impurity content (ppm by mass)	Surface density ( $\text{g}/\text{cm}^2$ )	Density at 0.1 to 0.15 m ( $\text{g}/\text{cm}^3$ )	$\alpha$	Comments
A	13 Mar 80	0°C	0.7	0.025–0.05	†	0.20	0.16	0.87	New snow, graupel
B	18 Mar 80	+2°C	0.3	0.04–0.06	0.022**	0.18	0.14	†	Melting snow, rounded needles
C	26 Mar 80	+2°C	>0.5	0.05–0.08 ( $z < 50 \text{ mm}$ ) 0.25–0.50 ( $z > 50 \text{ mm}$ )	0.059** Assumed to be the same for both cases	0.22	0.41	0.80	50 mm wet new snow over granular metamorphosed snow
C'	26 Mar 80	+2°C	>0.5	0.25–0.50					
D	28 Mar 80	+4°C	>0.5	0.13–0.25 ( $z < 30 \text{ mm}$ ) 0.25–0.50 ( $z > 30 \text{ mm}$ )	†	0.36	0.43	0.82	Granular meta- morphosed snow, 50 mm layer removed Granular snow, 30 mm new snow since 26 Mar
E	17 Apr 80	+13°C	>0.5	0.38–1.0	<500*** typical radius 10 to 15 microns	0.48	0.55	0.65	Dirty granular snow with natural surface
E'	17 Apr 80	+13°C	>0.5	0.38–1.0	†	0.51	0.55	0.64	Dirty granular snow 80 mm surface layer removed

\*0.5 times smallest dimension of typical particle.

\*\*Assumed to be graphitic carbon.

\*\*\*Dust.

† Not measured.

with dust and became contaminated with algae so that the carbon content could not be determined accurately. The amount of dust was estimated, however, by passing the sample through a 5  $\mu\text{m}$  millipore filter and measuring the total mass of trapped material with a sensitive balance scale. This gave an upper limit to the concentration of about 500 parts per million by mass. Visual examination of the dust under a microscope revealed particle diameters ranging from 5 to 300  $\mu\text{m}$  with a typical value between 20 and 30  $\mu\text{m}$ .

## OPTICAL RESULTS

The full albedo sequence is shown in Fig. 1. The individual points are indicated, and the thin solid lines connecting them represent a smoothed fit by hand. A 1% correction has been applied in order to account for the shadowing effect of the instrument. To avoid overlap, the scale for each successive curve has been displaced by 0.1 in  $\alpha_\lambda$ . The major source of uncertainty, indicated by the error bars, arises from fluctuations in the incident radiation field. At certain

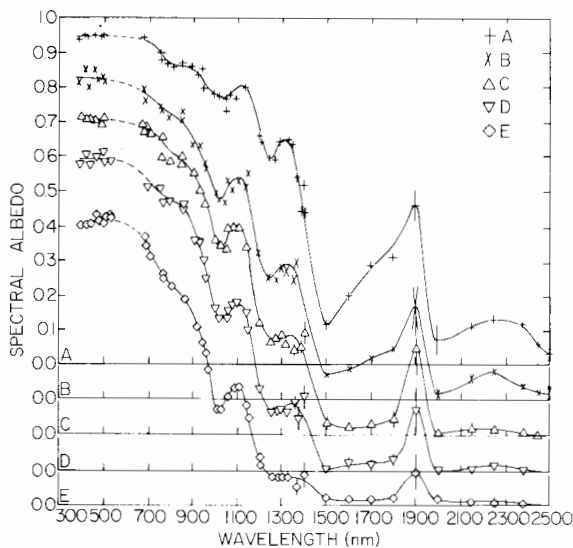


Fig. 1. Spectral albedo sequence of snow. Structural parameters of the snow for all cases are given in Table I. To avoid overlap, the scales for the different curves are displaced vertically as indicated by the 0.0 levels. The solid lines are approximate fits by hand to the data points.

wavelengths, notably 1900 nm, 2000 nm, and beyond 2450 nm, instrumental noise combined with low light levels produced significant additional contributions to the errors. Beyond 2500 nm albedos were too low to be measured reliably and are not reported. In cases where error bars are not shown, the uncertainties are less than or equal to the symbol dimensions. Although the data were corrected for variations in incident irradiance ( $F_{\text{in}}$ ) using the reference measurements, wavelength-integrated values give accurate corrections only if fluctuations are small; thus results are noisier from days when fluctuations in  $F_{\text{in}}$  were greater. The gap in  $\alpha_\lambda$  between 520 and 680 nm is due to a defect in the dispersion element of the photometer. The physical data associated with each albedo curve are listed in Table 1.

The albedo decreases at all wavelengths as the snow ages. Changes are strongest from 800 to 1900 nm in the infrared, and weakest at visible wavelengths. As indicated in Table 1, the general decrease is accompanied by an increase in the grain size and in impurity content. Between 380 and 700 nm only a slight change is noted from case A to case D, where no accumulation of impurities was detectable upon visual inspection, but a strong drop is evident between cases D and E when the snow became visibly dirty. Beyond 700 nm large changes took place even in the early stages of the sequence suggesting a much stronger dependence on grain size in the infrared.

An additional illustration of the effects of grain size is given in Fig. 2, where case C is compared with C'. These measurements were made within an hour of one another, case C being the albedo of the natural surface (6 cm of new wet snow over granular snow) and case C' being the albedo after the new layer was scraped off. The lack of data for C' at wavelengths less than 700 nm and greater than 1700 nm was caused by moisture condensation in the instrument near the end of the measurement sequence, which temporarily disturbed the performance characteristics of the electronics; however, the data reported were unaffected. The albedos of case C are uniformly higher than those of C' — from 5% at 700 nm to as much as 50% at 1300 nm. Since the snow had very low impurity levels in both cases, these differences would appear to be due mostly to the larger grain size in the underlying layer.

A more comprehensive representation of  $\alpha_\lambda$  versus

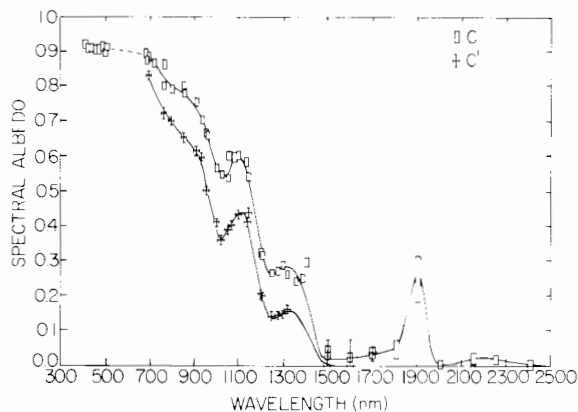


Fig. 2. Spectral albedos on 26 March 1980. Curve C is for the natural snow surface and curve C' is for the same surface with 50 mm of wet new snow removed. Structural parameters are given in Table 1. The solid lines are approximate fits by hand to the data points.

grain size is given in Fig. 3 for five different wavelengths over the entire series of observations. The horizontal error bars represent two-thirds of the total range in observed grain size about the estimated mean value. Assuming that grain size is approximately

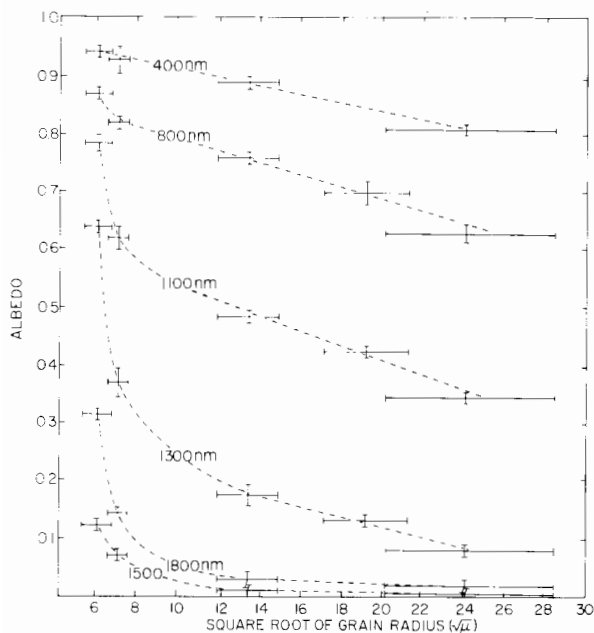


Fig. 3. Spectral albedos versus square root of grain radius ( $\mu\text{m}$ )<sup>1/2</sup> for cases A, B, D, C' and E' in order of increasing radius. The dashed curves are approximate fits by hand to the data points. The applicable wavelengths in nanometers are indicated.

normally distributed as suggested by the visual observations, the error limits then approximate the 95% confidence interval for the mean grain radius. The abscissa in Fig. 3 was chosen to be the square root of the grain radius in order to test the prediction by Bohren and Barkstrom (1974) that for visible wavelengths  $\alpha_\lambda = 1 - 5.96\sqrt{2\kappa_i r}$ , where  $r$  is the grain radius and  $\kappa_i$  is the absorption coefficient for pure ice. At 400 nm,  $\alpha_\lambda$  is indeed proportional to  $\sqrt{r}$ , but the slope of the curve implies that  $\kappa_i$  is about  $0.9 \text{ m}^{-1}$ , which is more than an order of magnitude larger than the observational results of Sauberer (1950). The remaining observational curves can also be compared with the numerical results of Wiscombe and Warren (1979) which cover the visible and infrared regions. For each of the five curves the observed albedo is lower than the predicted values and the variation with grain size is stronger, implying that an extra absorption mechanism is present in the snow pack. The linearity of the curves for grain radii greater than  $200 \mu\text{m}$  ( $\sqrt{r} = 14$ ) is not expected theoretically for pure snow, but the error bars are sufficiently large that some curvature could be present.

Additional absorption is probably provided by the increase in impurity levels in the snow. A comparison of the albedos for different impurity levels is shown in Fig. 4 for cases E and E'. Both curves describe visibly dirty homogeneous snow with the same grain size, except that in case E the uppermost 80 mm was observed to be significantly dirtier than the underlying layer. At visible wavelengths the albedos are

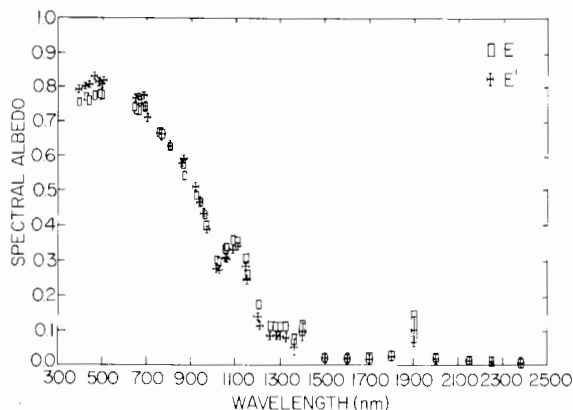


Fig. 4. Spectral albedos on 17 April 1980. Curve E is for the natural surface and curve E' is for the same surface with the dirty surface layer (80 mm) removed.

lower for the dirtier case (E) as expected, but at infrared wavelengths, the albedos are the same or slightly higher when the dirty surface layer is present. This will be discussed in more detail in the following section.

## DISCUSSION

In the infrared, observed albedos show a spectral distribution very similar to the calculations for pure snow of Choudhury (1979) and Wiscombe and Warren (1980). The actual values of  $\alpha_\lambda$ , however, are significantly lower than the theoretical predictions for the corresponding grain sizes, but the theory assumes clear sky conditions with a solar zenith angle of  $60^\circ$ , which gives somewhat higher albedos than for a diffuse incident field. In the visible the observations barely reach theoretically predicted levels for case A and decrease substantially with age down to about 0.8. Such low values are not achieved for pure snow even with unrealistically large grain radii of 10  $\mu\text{m}$ , and thus must be due to some other effect. As suggested in the previous section, an increase in impurity levels could account for this. Detailed modelling of the effects of impurities on snow albedo has been carried out by Warren and Wiscombe (1980). Their calculations show a strong influence in the visible but very little effect in the infrared. This is consistent with the present results, especially with the comparison between cases E and E', and is due to the sharp increase in the absorption coefficient of pure ice ( $\kappa_i$ ) with wavelength. In the visible  $\kappa_i$  is small compared to that of the impurities, but toward longer wavelengths it increases such that beyond about 900 nm it becomes comparable to absorption by soot or dust, and because of the much larger volume fraction of ice, the influence of the impurities become negligible. It appears, however, that the concentration of graphitic carbon inferred from the measured particle absorption coefficients was an order of magnitude too low to give agreement between observed and theoretical spectral albedos at visible wavelengths, although the amount of dust for case E may have been sufficient. Additional calculations are needed for the conditions particular to the present experimental results.

To test the accuracy of  $\alpha_\lambda$ , a comparison with  $\alpha$

was made by integrating the spectral albedo weighted by the incident irradiance using the relationship

$$\alpha_{\text{calc}} = \int \alpha_\lambda F_\lambda d\lambda / \int F_\lambda d\lambda, \quad (1)$$

where  $F_\lambda$  is the incident spectral irradiance at the surface. Since  $F_\lambda$  for cloudy skies could not always be obtained from the present data, the theoretical values of Choudhury and Chang (1980) for a solar elevation of  $35^\circ$  were used. The difference between observed total albedo ( $\alpha_{\text{obs}}$ ) and calculated albedo ( $\alpha_{\text{calc}}$ ) was always less than  $\pm 5\%$ . Much of the scatter, however, was probably due to variations in the cloud thickness. Such variations should result in systematic changes in the spectral distribution of  $F_\lambda$  which would give corresponding changes in  $\alpha_{\text{obs}}$  (Grenfell and Maykut 1977). To evaluate the importance of this effect on the agreement between total and calculated albedos, the differences  $\Delta\alpha = \alpha_{\text{obs}} - \alpha_{\text{calc}}$  were compared with measurements of the total incident shortwave irradiance ( $F_{\text{in}}$ ) for all cases where Kipp and Zonen radiometer data were taken. The results, plotted in Fig. 5, show a significant correlation between  $\Delta\alpha$  and cloudiness which appears to account for much of the scatter and suggests that the agreement is from 1 to 2% rather than 5%. In addition, because  $\Delta\alpha$  is small for all the recorded values of  $F_{\text{in}}$  and passes through zero near the middle of the observed range, the calculations of  $F_\lambda$  of Choudhury and Chang (1980) appear to represent the present conditions quite well.

Figure 5 shows that as the light levels increase in response to decreasing cloud thickness,  $\alpha_{\text{obs}}$  decreases

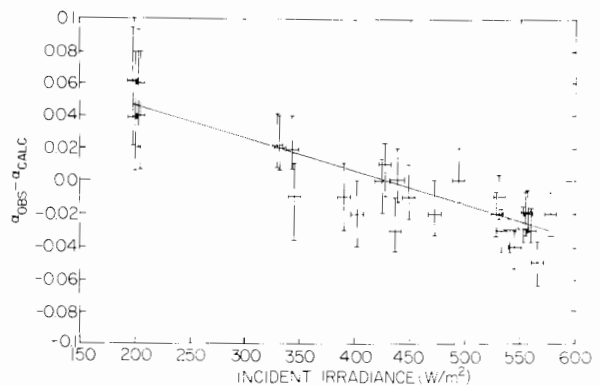


Fig. 5. The difference between observed and calculated integrated albedos ( $\Delta\alpha$ ) versus incident irradiance. The straight line is a least squares fit to the data points.

with respect to  $\alpha_{\text{calc}}$ . This behaviour is consistent with the expectation that for a thinner cloud cover the relative contribution of the near-infrared to the total incident radiation field is larger, weighting the integral in the numerator of eqn. (1) more heavily at longer wavelengths where spectral values are lower. A least squares linear fit to the data points, indicated by the solid line in Fig. 5, gives  $\alpha_{\text{obs}} = \alpha_{\text{calc}} - 0.2935 F_{\text{in}} + 0.0863$  with a correlation coefficient of 0.92. This relationship does not appear to be sensitive to the effects of grain size or impurities on  $\alpha_{\lambda}$ , although observations were not obtained over a wide enough range of cloud conditions for any particular snow state to make a more definitive test.

## ACKNOWLEDGMENTS

This work was made possible by continued support from the Office of Naval Research, Arctic Program under Contract N00014-76-C-0234.

## REFERENCES

- Astrom, R.W. (1973), Extinction and absorption coefficients of the atmospheric aerosol as a function of particle size. *Beitr. Phys. Atmos.*, 46: 223–234.
- Chen, C.F. and Barkstrom, B.R. (1974), Theory of the optical properties of snow, *J. Geophys. Res.*, 79(30): 4527–4535.
- Chen, C.F. and Beschta, R.L. (1979), Snowpack albedo and snow density, *Cold Reg. Sci. Tech.*, 1(1): 47–50.
- Chern, N.N. and Koptev, A.P. (1969), O spektral'nom albedo snezhnoledyanogo pokrova (Spectral albedo of a snow ice cover), *Problemy Arktiki i Antarktiki*, 31: 79–83.
- Coudhury, B.J. (1979), Thermal conditions in a snowpack I: The energy balance components, *Computer Sciences Corp. Tech. Rep. 79/6006*, 39 pp.
- Coudhury, B.J. (1980), personal communication.
- Coudhury, B.J. and Chang, A.T.C. (1980), The albedo of partially cloudy skies, *NASA Tech. Memo.* 79-247, 25 pp.
- Coudhury, B.J. (1981), A visible and near-infrared scanning radiometer for ground measurements of spectral albedo and snow grain size under various conditions, *J. Glaciol.* (in press).
- Grenfell, T.C. and Maykut, G.A. (1977), The optical properties of ice and snow in the Arctic Basin, *J. Glaciol.*, 18 (80): 445–463.
- Holmgren, B. (1963, unpublished). [Changes of albedo on the Devon Island ice cap, paper presented at 4. Internationale Polartagung der Deutschen Gesellschaft für Polarforschung e.V., 1963.] Cited in Mellor (1977)
- Engineering properties of snow, *J. Glaciol.*, 19 (81): 15–66.
- Kuhn, M. and Siogas, L. (1978), Spectroscopic studies at McMurdo, South Pole, and Siple stations during the austral summer 1977–78, *U.S. Antarctic J.*, 13: 178–179.
- Liljequist, G.W. (1956), Energy exchange of an antarctic snow-field. Shortwave radiation (Maudheim, 71°03'S, 10°56'W). Norwegian–British–Swedish Antarctic Expedition, 1949–52, *Scientific Results*, 2(1A).
- Lin, C., Baker, M. and Charlson, R.J. (1973), Absorption coefficient of atmospheric aerosol: A method for measurement, *Appl. Optics*, 12: 1356–1363.
- O'Brien, H.W. and Munis, R.H. (1975), Red and near-infrared spectral reflectance of snow, *U.S. Army CRREL Res. Rep.* 332, 18 pp.
- Roessler, D.M. and Faxvog, F.R. (1980), Optical properties of agglomerated acetylene smoke particles at 0.5145  $\mu\text{m}$  and 10.6  $\mu\text{m}$  wavelengths, *J. Opt. Soc. Am.*, 70(2): 230–235.
- Rosen, H., Hansen, A.D.A., Gundel, L. and Novakov, T. (1978), Identification of the optically absorbing component in urban aerosols, *Appl. Optics*, 24: 3859–3861.
- Sadler, M., Charlson, R.J., Rosen, H. and Novakov, T. (1981), An intercomparison of the integrating plate method and laser transmission methods for determination of aerosol absorption coefficients. *Atmospheric Environment* (in press).
- Sauberer, F. (1950), Die spektrale Strahlungsdurchlässigkeit des Eises, *Wetter und Leben*, Jahrg. 2, Heft 9/10, p. 143–197.
- Warren, S.G. and Wiscombe, W.J. (1980), A model for the spectral albedo of snow. II. Snow containing atmospheric aerosols, *National Center for Atmospheric Research, NCAR/0304/80-2; J. Atmos. Sci.*, 37(12) (in press).
- Weiss, R.E., Waggoner, A.P., Charlson, R.J., Thorsell, D.L., Hall, J.S. and Riley, L.A. (1979), Studies of the optical, physical, and chemical properties of light absorbing aerosols, *Proc. Conf. on Carbonaceous Particles in the Atmosphere*, Lawrence Radiation Laboratory, Berkeley, California.
- Wiscombe, W.J. and Warren, S.G. (1980), A model for the spectral albedo of snow. I. Pure snow, *National Center for Atmospheric Research, NCAR/0304/79-09; J. Atmos. Sci.*, 37(12) (in press).